

Single electron transistor at room temperature fabricated on the large area surface of hydrogenated diamond like carbon thin film

Nihar R. Ray^{*||}, Jagannath Datta[§], Hari S. Biswas[¶], Pintu Sen[†] and Kousik Bagani^{||}

^{*}Center for Nano-Science and Surface Physics Project, ^{||}Surface Physics Division, Saha Institute of Nuclear Physics, Kolkata -700 064, India

[§]Analytical Chemistry Division, BARC, Variable Energy Cyclotron Center, Kolkata-700 064, India

[¶]Department of Chemistry, Surendranath College, Kolkata-700 009

[†]Department of Physics, Variable Energy Cyclotron Center, Kolkata-700 064, India

Introduction

The single electron transistor (SET) switches on and off every time an electron is added to conducting island, called coulomb blockade (CB), isolated from two metallic leads, source (S) and drain (D), by insulator, called tunnel barrier (TB)¹. In order to avoid thermally induced random tunneling events, the minimum size of CB has to be smaller than ~ 1 nm for room temperature (RT) operation of SET². The present conventional microfabrication process limits the size of CB within a few tens of nm^{3, 4}. The nature of the CB -metallic nanostructures, semiconducting, or quantum dot – is irrelevant for creation of SET, in first order approximation². Here we show SET at RT, operated on macroscopic system-the two-dimensional (2D) large area (0.012 m \times 0.012 m) surface of our hydrogenated diamond like carbon (HDLC) thin film⁵⁻⁹. Our results, free from the limitation of lowering the size of CB in sub-nanometer range with the existing unprofitable process^{3, 4}, are consistent with the theoretical results^{1, 10, 11}, and will be relevant for real application² at RT in a practical size device.

*Corresponding author. E-mail: niharranjan.ray@saha.ac.in

Experiments

The experimental data of SET at RT, based upon diamond like carbon (DLC) is not reported in the literature¹²⁻¹⁴. The HDLC thin film grown onto large area substrate Si (100), behaves as a 2D graphitic film, having both p-type and n-type surface conduction⁹.

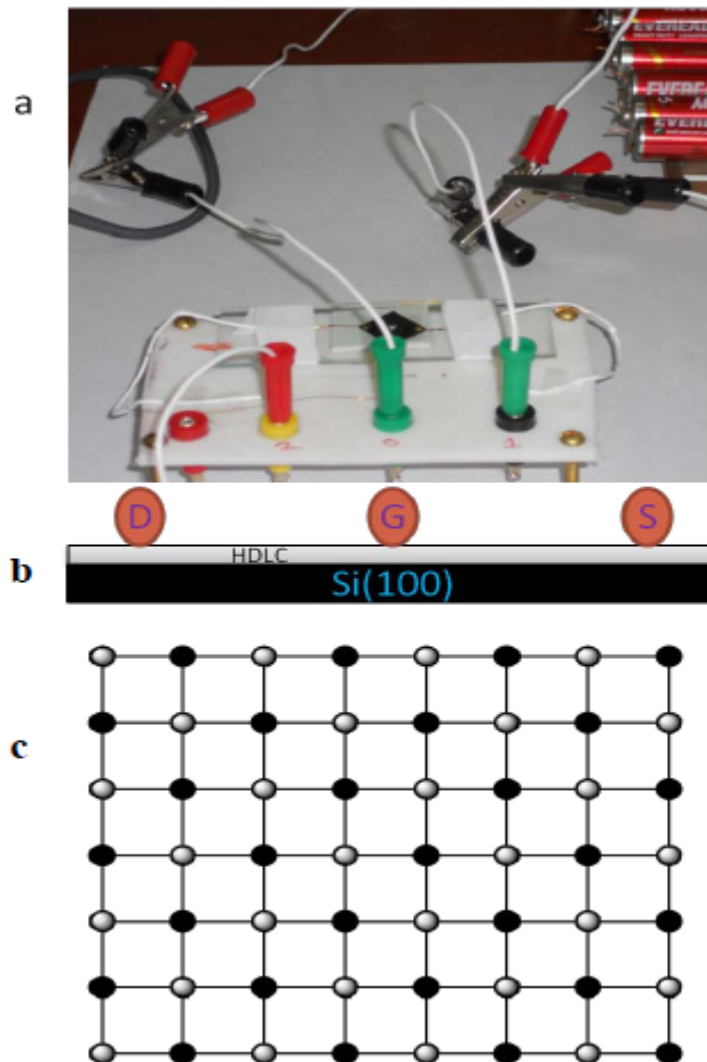


Figure 1. Picture and Schematic layout of sample. a, A picture of three ohmic contacts on the surface of HDLC thin film and the connecting wires from these contacts. b, A schematic view of layers of Si(100) substrate, thin film of HDLC and three ohmic contacts: source (S), gate (G) and drain (D), corresponding to three

contacts in the picture, onto the surface of HDLC sample. c, A schematic view of the top of HDLC surface; solid circles represent non-conducting (sp^3 C-H) carbons, hollow circles represent conducting (sp^2 C=C) carbons, and the solid lines represents interconnections between solid and hollow circles indicating coherent domains of sp^2 and sp^3 .

A picture of ohmic contacts of Cu- source, gate and drain onto the HDLC surface^{9, 14} (see Fig. 1a), layout of HDLC (see Fig. 1b), and schematic view of the top HDLC surface (see Fig. 1c) are shown. The top view shows coherent domains of sp^3 C-H (non-conductor) and sp^2 C=C (conductor) carbons and thus indicating resistive nature of the HDLC surface¹⁵. A Keithley 2635 source meter is used to measure the sheet resistance and I-V characteristics on the HDLC surface⁹ at RT (295K). A confocal Micro-Raman spectrometer is used to measure Raman spectra of the HDLC samples⁵⁻⁹. In order to reduce the size of the domain of conducting (sp^2 C=C) carbons isolated by the domains of non-conducting (sp^3 C-H) carbons, we have applied electrochemical method¹⁶ for hydrogenation of sp^2 C=C bond on the pristine HDLC surface, and thus produce electrochemically hydrogenated diamond like carbon (ECHDLC) surface.

Results and Discussion

The typical sheet resistance of the ECHDLC surface \approx 5-8 G Ω for sourcing current 1000 nA is much larger than that \approx 75 M Ω of pristine HDLC surface for sourcing current 100 nA. The typical I-V characteristics between source and drain for pristine HDLC and ECHDLC surface (see Fig. 2a) respectively are consistent with the results of

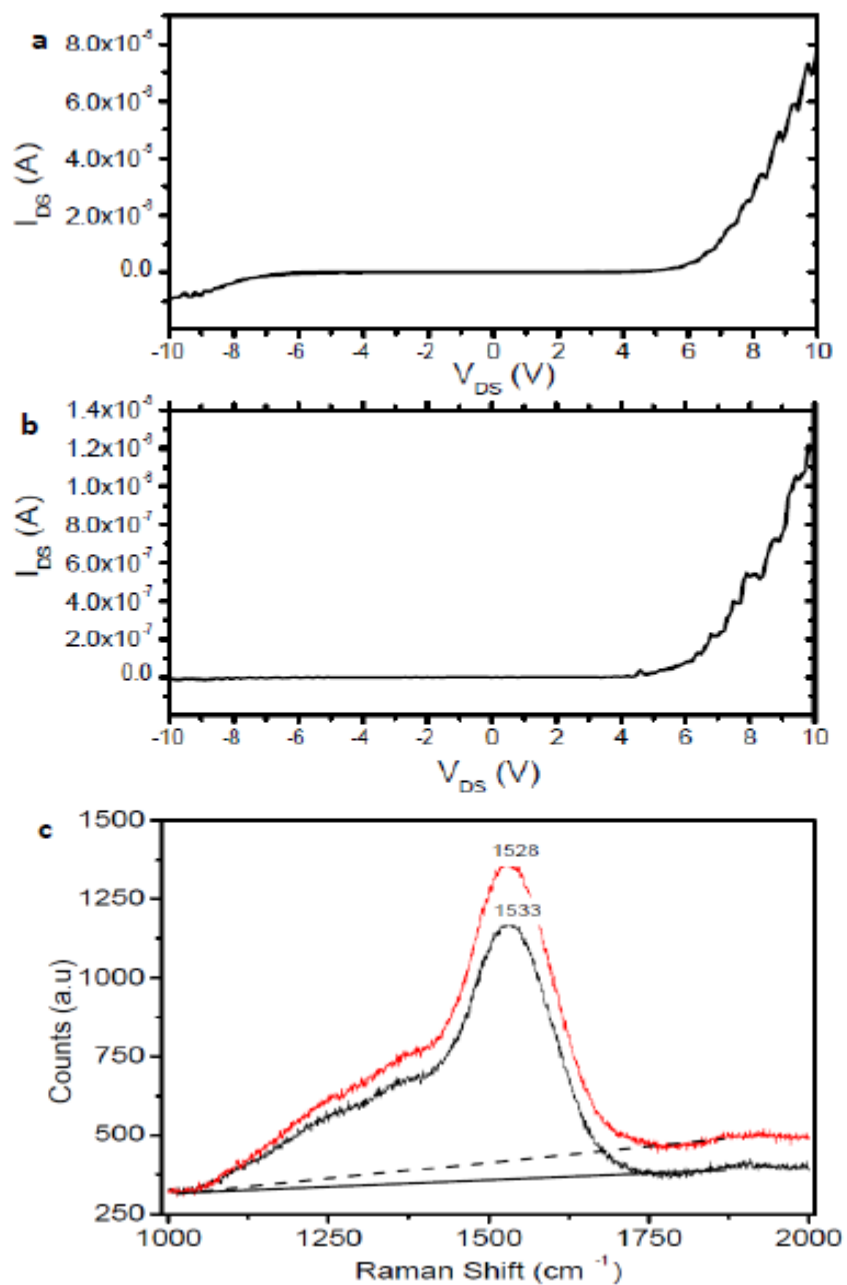


Figure 2. Current (I) vs. Voltage (V) characteristic and Raman spectrum of sample.
a, Typical current (I_{DS}) vs. voltage (V_{DS}) characteristic of the pristine HDLC surface of area $0.012 \text{ m} \times 0.012 \text{ m}$.
b, Typical current (I_{DS}) vs. voltage (V_{DS}) characteristic of the ECHDLC surface of area $0.012 \text{ m} \times 0.012 \text{ m}$.
c, Typical first order Raman spectra of pristine HDLC (black) and ECHDLC (red) samples.

sheet resistances. The I-V characteristics (see Fig. 2a) show no hysteresis during measurements by increasing and decreasing drain voltage. The typical first-order Raman spectra of pristine HDLC and ECHDLC samples (see Fig. 2b) give sp^3 content, estimated from the position of G-peak ($\omega_G, \mu m^{-1}$) using the equation, sp^3 content = $0.24 - 48.9 (\omega_G - 0.1580)$, derived in our earlier works⁶. Enhancement of sp^3 C-H content, from 47% (for pristine HDLC) to 49% (for ECHDLC) is observed. Moreover, we observe, increase of the slope of photoluminescence background¹⁷ in the typical Raman spectrum of ECHDLC sample w.r.t that of pristine HDLC (see Fig. 2b) which clearly indicates increase of bonded hydrogen. Estimation of the ratio of slope (m) and intensity of G-peak (I_G) of the Raman spectra i.e. m/I_G gives approximately 1.5% increase of sp^3 C-H bonds in the ECHDLC sample. The indigenous technique for enhancement of hydrogenation of pristine HDLC surface, and hence to reduce the size of the isolated domains of conducting carbons (sp^2 C=C), is reported in the present work for the first time.

The typical results on drain-source current (I_{DS}) vs. drain-source voltage (V_{DS})/time (t), and drain-source conductance (σ_{DS}) vs. drain-source voltage (V_{DS}) at different gate voltage (V_G) respectively, are shown in Figure 3. In the pristine HDLC surface, we observe quasi-periodic oscillation of hole current (I_{DS}^h) and conductance (σ_{DS}^h) for $V_G = +7.5$ v (see Fig. 3a and b) and $V_G = +9$ v (see Fig. 3c and d) respectively with “step-like” structure in I-V/conductance characteristic; the conductance value is approximately three orders lower than quantum conductance (e^2/h), and increases with V_{DS} . Similarly, in the ECHDLC surface, we observe quasi-periodic oscillation of electron current (I_{DS}^e) and conductance (σ_{DS}^e) for $V_G = -7.5$ v (see Fig. 3e and f) and $V_G = -9$ v (see Fig. 3g and h)

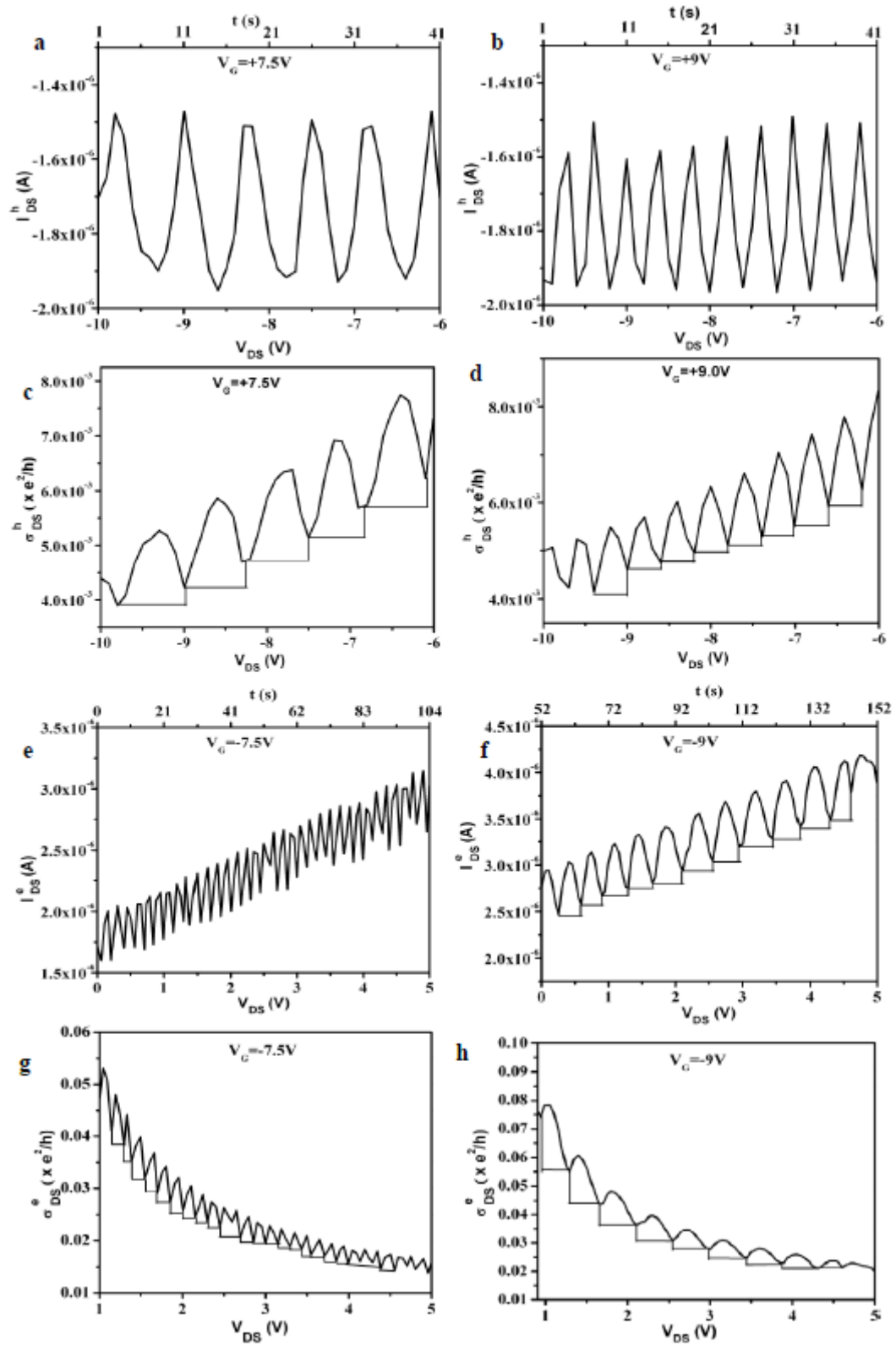


Figure 3. Current (I_{DS}) vs. Voltage (V_{DS})/Time (t) and Conductance (σ_{DS}) vs. Voltage (V_{DS}) for a given Gate Voltage (V_G). a, I_{DS}^h vs. V_{DS} and I_{DS}^h vs. t for $V_G = +7.5$ v. b, σ_{DS}^h vs. V_{DS} for $V_G = +7.5$ v. c, I_{DS}^h vs. V_{DS} and I_{DS}^h vs. t for $V_G = +9.0$ v. d, σ_{DS}^h vs. V_{DS} for $V_G = +9.0$ v. e, I_{DS}^e vs. V_{DS} and I_{DS}^e vs. t for $V_G = -7.5$ v. f, σ_{DS}^e vs. V_{DS} for $V_G = -7.5$ v. g, I_{DS}^e vs. V_{DS} and I_{DS}^e vs. t for $V_G = -9.0$ v. h, σ_{DS}^e vs. V_{DS} for $V_G = -9.0$ v.

respectively with “step-like” structure in I-V/conductance characteristic; here the conductance value is approximately two orders lower than e^2/h , and decreases with V_{DS} . For the estimation of single electron/hole capacitance (C_e / C_h) and no. of charges (N) transferred to the CB, we measure increase of voltage (ΔV) between two peaks, say peak i to peak (i+1) in I_{DS} vs. V_{DS} graphs, and current increase (ΔI) with time (Δt) corresponding to peak (i+1) in I_{DS} vs. t graphs in Fig. 3. From these measured values, we estimate, $\Delta Q = \Delta I \times \Delta t = Ne$; single electron/hole capacitance (C_e / C_h) = $e/\Delta V$.

Table 1 Electrical parameters for SET at RT

Parameter	Material			
	Pristine HDLC surface		ECHDLC surface	
	$V_G = +7.5$ V	$V_G = +9$ V	$V_G = -7.5$ V	$V_G = -9$ V
N_h	0.825E+13	0.451E+13	-	-
N_e	-	-	0.585E+13	1.056E+13
C_h (F)	2E-19	4E-19	-	-
C_e (F)	-	-	1E-18	6E-19
ΔV (V)	0.810	0.401	0.158	0.300
ΔI (A)	0.432E-6	0.355E-6	0.450E-6	0.552E-6
Δt (s)	3.06	2.03	2.08	3.06

In Table 1 we give measured electrical parameters relevant for SET at RT on the surface of 2D HDLC thin film. In order to give a plausible physical explanation for the measured results in Table 1, we may assume a simple model: between S and D separated by macroscopic distance (~ 0.01 m) on $0.012 \text{ m} \times 0.012 \text{ m}$ HDLC surface, there are large numbers of conducting (sp^2 C=C) carbon as CB separated by large numbers of non-conducting (sp^3 C-H) carbon as TB and CB and TB exist coherently⁸ (see Fig. 1c). The increase of voltage ΔV between S and D for a given gate voltage V_G , when a single electron (hole) starts from S, passing through all CBs and TBs with finite tunneling probability ultimately reaches D, there is a peak in current/conductance. The next electron does not start from S until the tunneling of previous electron is completed, and hence there is a time-gap between the electrons reaching at D, resulting in a fall of current in I-V graph during that time-gap. Now, if we assume, total numbers of CBs / TBs are 10^{13} , and each CB contributes only one conducting electron, then total equilibrium number of conducting electrons in all CBs, between S and D, will be 10^{13} . Now during electron (hole) tunneling process between S and D with finite probability, the increase of number of electron in each CB will be $(1 \pm \epsilon)$, and that in all CBs will be $(1 \pm \epsilon) 10^{13}$. If we assume $0 < \epsilon < 1$, then we can say that the measured values of N_h and N_e (see Table 1), are reasonable. Therefore our results, that periodic peaks in I-V and conductance characteristics correspond to average number of electrons in a single CB is not an integer but $(1 \pm \epsilon)$, are consistent with theory^{1,10,11} wherein average number of electrons in a single CB is $(N+1/2)$. Moreover, height of the steps in I-V/conductance characteristics, depending upon gate voltage V_G , are not equal (see Fig. 3) but that for single CB, the corresponding steps are equal¹⁸. The values of C_e are a few times larger

than that of C_h (see Table 1), but the order of magnitude for both values tells us that the diameter of CB is ~ 1 nm or less and the corresponding charging energy of several hundred meV (see Table 1) seems to be plausible². Therefore the measured parameters (N_h , N_e , C_h , C_e , ΔV & ΔI) in Table 1 are reasonable for SET at RT according to basic theory of SET^{1, 2, 10, 11}. Considering the result Δt , that a single electron travels large numbers of CBs/TBs in time of seconds (see Table 1), we can say that sensitivity for detection of ‘single electron event’ or that for ‘counting of electrons’ should be high in our SET at RT. Thus our SET at RT seems to be relevant for practical applications in the future development of solid-state electrometer¹⁹, electron pumps²⁰, artificial neural network^{2, 21}.

Conclusion

We conclude that charge quantization at RT and hence SET at RT on the large surface area of our 2D HDLC thin film, wherein there are \sim ten-trillion CBs separated by approximately same numbers of TBs with sub-nanometer size of each, and corresponding capacitance in the range of attofarad, respectively, is produced and operational.

.....

References

1. Kastner, M.A. The single electron transistor and artificial atoms. *Ann.Phys. (Leipzig)*. **9**, 885-894 (2000).
2. Grabert, H. & Devoret, M.H. in *Single Charge Tunneling* (eds Grabert, H. & Devoret, M.H.) Ch. 1 (NAT ASI Ser., Plenum, New York, 1992).

3. Matsumoto, K., Tshi, M., Segwa, K & Oka, Y. Room temperature operation of a single electron transistor made by the scanning tunneling microscope nanooxidation process for TiO_x/Ti system. *Appl. Phys. Lett.* **68**, 34-36 (1996).
4. Karre, P.S., Bergstrom, P.L., Mallick, G. & Karna, P.S. Room temperature operational single electron transistor fabricated by focused ion beam deposition. *J. Appl. Phys.* **102**, 024316-1-4 (2007).
5. Ray, N.R. & Iyengar, A.N.S. Proc. Of the Sixth Int. Conf. on Reactive Plasmas and 23rd Symposium on Plasma processing, 24-27 January 2006, Matshushima/Sendai, Japan, 2006, edited by R Hatakeyama and S.Samukawa (ICRP-6/SPP-23), p-583.
6. Singha, A., Ghosh, A., Roy, A. and Ray, N.R. Quantative analysis of hydrogenated diamondlike carbon films by visible Raman spectroscopy. *Jour. Appl. Phys.* **100**, 044910-1-8 (2006).
7. Biswas, H.S. *et al.* Covalent immobilization of protein onto a functionalized hydrogenated diamond-like carbon substrate. *Langmuir* **26**, 17413-17418 (2010).
8. Datta, J., Ray, N.R., Sen, P., Biswas, H.S., Vogler, E.A. Structure of hydrogenated diamond like carbon by Micro-Raman spectroscopy. *Materials Letters* **71**, 131-133 (2012).
9. Ray, N.R., Datta, J., Biswas, H.S. and Datta, S. Signature of misoriented bilayer graphenelike and graphanelike structure in the hydrogenated diamond-like carbon film. *IEEE Transactions on Plasma Science* **40**, 1789-1793 (2012).
10. Kulik, I. O. & Shekhter, R.I. Kinetic phenomena and charge discreteness effects in granular media. *Sov.Phys. JETP.* **41**, 308-316 (1975).

11. Glazman, L.I. Single electron tunneling. *Jour. Of Low Temp. Phys.***118**, 247-269 (2000).
12. Wu, Y. *et al.* High frequency scaled graphene transistors on diamond like carbon. *Nature* **472**, 74-78 (2011).
13. Angus, J.C. and Hayman, C.C. Low-pressure, metastable growth of diamond and “diamondlike” phases. *Science* **241**, 913-921(1988).
14. Tsugawa, T. *et al.* High-performance diamond surface-channel field-effect transistors and their operation mechanism. *Diamond and Related Materials.* **8**, 927-933 (1999).
15. Savchenko, A. Transforming graphene. *Science* **323**, 589-590 (2009).
16. Maier, F., Riedel, M., Mantel, B., Ristein, B., and Ley, L. Origin of surface conductivity in diamond. *Phys. Rev. Lett.* **85**, 3472-3475 (2000).
17. Marchon, B., *et al.* Photoluminescence and Raman spectroscopy in hydrogenated carbon films. *IEEE Trans. Magn.* **33**, 3148-3150 (1997).
18. Devoret, M.H., Esteve, D., Urbina, C. Single-electron transfer in metallic nanostructures. *Nature* **360**, 547-553 (1992).
19. Devoret, M.H. and Schoelkopf, R.J. Amplifying quantum signals with the single-electron transistor. *Nature* **406**, 1039-1046 (2000).
20. Keller, M.W., Eichenberger, A.L., Martinis, J.M. and Zimmerman, N. M. A capacitance standard based on counting electrons. *Science* **285**, 1706-1709 (1999).
21. Hafsi, B., Boubaker, A., Krout, I. and Kalboussi, A. Simulation of single electron transistor inverter neuron: memory application. *Int.J. of Information and Computer Science* **2**, 8-15 (2013).

Acknowledgements

One of the authors (NRR) thanks Dept. of Atomic Energy, Govt. of India for funding during XI plan period to create the experimental facilities for carrying out the present work. We thank Mr. S. S. Sil and Mr. U. S. Sil for technical help and Dr. S Chattopadhyay and Dr. S Bhuia for fruitful scientific discussions.